RSC Advances

RSC Advances

www.rsc.org/advances

ROYAL SOCIETY OF CHEMISTRY

www.rsc.org/advances

Graphical Abstract:

Series of highly efficient phosphorescent organic light-emitting diodes (PhOLEDs) based on two iridium complexes (**1** and **2**) constructed by the N^C^N-coordinated terdentate ligands have been achieved. They exhibit the high peak power efficiency (PE) and external quantum efficiency (EQE) values of 35.5 lm W^{-1} & 15.8 % for blue-green emission, 47.4 lm W^{-1} & 16.7 % for green emission, which maintain the high level of 19.2 lm W^{-1} & 14.5 % and 30.6 lm W^{-1} & 16.1 % at rather high and practical luminance of 500 cd m^{-2} with the low driving voltages of less than 6 V. The appropriate selection of a prominent electron-transport molecule TPBi as a host to matching the dopant molecules (**1** or **2**) that possess the obvious hole-transport ability is critical in the remarkable EL-performance improvement on previous reports.

ARTICLE TYPE

High Performance Blue-Green and Green Phosphorescent OLEDs Based on Iridium Complexes with N^C^N-Coordinated Terdentate Ligands

Dong Chen, Liang Han, Dong Liu, Kaiqi Ye, Yu Liu*, Jingying Zhang* and Yue Wang

Highly efficient phosphorescent organic light-emitting diodes (PhOLEDs) based on two iridium complexes constructed by the N^C^N-coordinated terdentate ligands (also called pincer ligands) have been achieved. They exhibit the high peak power efficiency (PE) and external quantum efficiency (EQE)
10 values of 35.5 lm W^{-1} & 15.8 % for blue-green emission, 47.4 lm W^{-1} & 16.7 % for green emission, which maintain the high level of 19.2 lm W^{-1} & 14.5 % and 30.6 lm W^{-1} & 16.1 % at rather high and practical luminance of 500 cd m^{-2} with the low driving voltages of less than 6 V. These values show almost a twofold enhancement over the most efficient PhOLEDs based on the pincer iridium complexes ever reported. Here, the appropriate selection of a prominent electron-transport molecule TPBi as a host
15 to matching the dopant molecules (**1** or **2**) that possess sufficient hole-transport ability is critical in the remarkable EL-performance improvement on previous reports. We will present a comprehensive investigation that not only encompasses the conventional thermal, photophysical and electrochemical properties of both complexes, but also emphatically studies the charge carrier injecting/transporting and electroluminescent (EL) characteristics of two phosphorescent emitters doped in different host.

20 Introduction

As we known, a 100% internal quantum efficiency (IQE) of electrophosphorescence can be achieved by harvesting both electrogenerated singlet and triplet excitons for emission.[1] Iridium complexes composed of cyclometallated ligands are
25 promising phosphorescent materials and have been intensively studied for phosphorescent organic light-emitting diodes (PhOLEDs).[2] For the larger enhancement in device efficiency, many research were focused on developing a vast range of derivatives of the Ir(C^N)₃ and Ir(C^N)₂(L^X) structural classes
30 {C^N = anionic bidentate cyclometallating ligands such as 2-phenylpyridine (ppy); L^X = anionic ancillary ligands such as acetylacetone (acac)}.[3] In particular, Ir(ppy)₃ is used widely in organic light-emitting diodes (OLEDs) owing to its high quantum yields and thermal stability. Actually, the iridium complexes
35 composed of tridentate cyclometalated ligands such as the type of N^C^N-coordinating ligands, also called pincer ligands,[4] are believed to possess better thermal stability than those with two bidentate ligands above. It is beneficial for fabricating OLEDs and their stability. However, up to now, there are rare pincer Ir
40 complexes being applied to fabricating OLEDs, which generally showed moderate efficiencies {≈ 5 lm W^{-1} (Power Efficiency, PE) or 8 % (External Quantum Efficiency, EQE) for blue-green emission, ≈ 10 lm W^{-1} or 10 % for green or orange emission} and rather high driving voltages (> 10 V reaching the luminance of
45 500 cd m^{-2}).[4b,c]

On the other hand, for the most PhOLEDs with the doping system based on the fluorescent host and the phosphorescent dopant emitter, the hole and/or electron injection into the highest occupied molecular orbital (HOMO) and/or the lowest
50 unoccupied molecular orbital (LUMO) of the dopant and then direct charge recombination in the dopant, is considered more efficient for the formation of excitons than host-to-dopant energy transfer.[5] Obviously, this direct charge recombination process can eliminate not only the need to overcome the large energy barriers
55 between the charge transport layers and the emitting layer (EML) resulted from the wide HOMO−LUMO gap of the host, but also the energy losses during the exothermic host-dopant energy transfer process. Generally, the phosphorescent emitting molecules possess certain mobility for hole and/or electron,
60 which thus can undertake a portion of the transporting task for one type or both charge carrier (hole and electron) in addition to the host molecules and ensure the balanced charge fluxes.[6] As such, it is indeed an effective and easy approach to achieve high performance PhOLEDs by constructing and assembling carrier
65 matched and balanced host/dopant pair in EML, where the hole and electron are transported through the host and dopant molecules respectively, instead of by host only. This will effectively avoid the complex design and synthetic route for developing new ingenious hosts and/or phosphorescent emitters
70 possessing the bipolar transporting ability. However, the current studies for exploring such bipolar host-dopant system are rare and the desired device performance haven't been realized yet.[7]

In this contribution, we report two highly efficient PhOLEDs

based on two [Ir(N^C^N)(N^C)X]-type dopant emitters (Scheme 1) that are composed of one terdentate cyclometallating ligand, one bidentate cyclometallating ligand, and one monodentate ligand: **Ir(F$_2$dpyb)(ppy)Cl** (complex **1**) and **Ir(dpyx)(ppy)Cl**

5 (complex **2**) (F$_2$dpyb = 2-(2,4-difluoro-5-(pyridin-2-yl)phenyl)pyridine; dpyx = 2-(2,4-dimethyl-5-(pyridin-2-yl)phenyl)pyridine) (Fig. 1 inset).[4c] They show very high peak PE and EQE values of 35.5 lm W^{-1} & 15.8 % for blue-green emission from **1**, 47.4 lm W^{-1} & 16.7 % for green emission from

10 **2**, which maintain the high level of 19.2 lm W^{-1} & 14.5 % and 30.6 lm W^{-1} & 16.1 % at rather high and practical luminance of 500 cd m^{-2} with the low driving voltages of less than 6 V. To the best of our knowledge, they are the highest EL efficiency values for the PhOLEDs ever reported adopting the pincer iridium

15 complexes as the phosphorescent emitters, and show almost two times higher than the previously reported results.[4] Such remarkable enhancement of EL performance is attributed to the carefully selecting a classical electron-transporting (ET)-type molecule 1,3,5-tris(N-phenylbenzimidazol-2-yl)benzene (TPBi)[7a]

20 as the host material, which well matched the inherent hole-transporting (HT) character of two phosphorescent emitter **1** and **2** used here. This bipolar host-dopant system possessing highly complementary HT and ET ability can promote hole injection/transport through phosphorescent molecules and

25 electron injection/transport through TPBi molecules, and then lead to direct charge recombination on the dopant. This process can improve the recombination probability because both the holes and the electrons can migrate freely and the excitons form not only at the interfaces, but can diffuse evenly throughout the

30 EMLs,[5f,g] which could suppress the triplet-triplet annihilation (TTA)[8] as much as possible within the EMLs, thus enhancing the device efficiency. Hence, these iridium complexes with terdentate ligands no longer are overlooked, which even become the intense research activity in testing phosphors for OLEDs parallels to the

35 bibentate ligand-based iridium complexes, due to their improved EL performance as well as the desired thermal stability.

We will present a comprehensive investigation that not only encompasses the conventional thermal, photophysical and electrochemical properties of both compounds, but also

40 emphatically studies the charge carrier injecting/transporting and electroluminescent (EL) characteristics of the thermal deposited films based on the emitter **1** and **2** doped in different host.

Experimental section

General information

45 Materials obtained from commercial suppliers were used. Anhydrous hexane was distilled with sodium benzophenone ketyl under nitrogen atmosphere and degassed by the freeze-pump-thaw method. All glasswares, syringes, magnetic stirring bars and needles were dried in a convection oven for at least 4 hours.

50 Reactions were monitored with thin layer chromatography (TLC). Commercial TLC plates (Silica gel 60 F254, Merck Co.) were developed and the spots were seen under UV light at 254 and 365 nm. Silica column chromatography was done with silica gel 60 G (particle size 5~40 μm, Merck Co.). ^{1}H NMR spectra were

55 recorded on a Bruker AVANCE 300 MHz spectrometer with tetramethylsilane as an internal standard. Mass spectra were

measured on a GC/MS mass spectrometer. Elemental analyses were performed on a flash EA 1112 spectrometer. Absorption spectra were obtained using a Shimadzu UV-2550 UV-vis

60 spectrometer. PL spectra were recorded on a Perkin-Elmer LS-55 fluorescence spectrometer with a Xe arc lamp excitation source. All solvents were degassed via three freeze-pump-thaw cycles. Electrochemical measurement was performed with a BAS 100W Bioanalytical electrochemical work station, using Pt working

65 electrode, platinum wire as auxiliary electrode, and a porous glass wick Ag/Ag$^+$ as reference electrode. The voltammograms were referenced to the ferrocene/ferrocenium couple and the scan rate was 100 mV S^{-1}. Due to the limitation[9] in measuring reduction potentials in the range of -2.7 V to -3.5 V in CH$_2$Cl$_2$, we obtained

70 only the oxidation potential for (ppy)$_2$Ir(dipig), and no reduction wave was detected within the electrochemical window of dichloromethane. The highest occupied molecular orbital (HOMO) and the lowest unoccupied molecular orbital (LUMO) energy levels of the complex were calculated from the cyclic

75 voltammetry (CV) data together with the absorption spectrum.

Device fabrication and measurement

Before device fabrication, the emitting complexes of **1** and **2**, 1,4-bis[(1-naphthylphenyl) amino]-biphenyl (NPB), 4,4',4''-tri(*N*-carbazolyl) triphenylamine (TCTA), 4,4'-*N,N'*-

80 dicarbazolylbiphenyl (CBP) and TPBi were prepared and purified by sublimation, and ITO glass substrates were pre-cleaned carefully and treated by UV/O$_3$ for 2 min. The devices were prepared in vacuum at a pressure of 5 × 10^{-6} Torr. All organics were thermally evaporated at a rate of 1.0 Å S^{-1} at a base pressure

85 of around 3.5 x 10^{-4} Pa. A LiF layer (0.5 nm) was deposited at a rate of 0.2 Å S^{-1}. The finishing Al electrode (cathode) was deposited at a rate of 10 Å S^{-1} in another chamber. The thicknesses of the organic materials and the cathode layers were controlled using a quartz crystal thickness monitor. The electrical

90 characteristics of the devices were measured with a Keithley 2400 source meter. The EL spectra and luminance of the devices were obtained on a PR650 spectrometer. All the devices fabrication and device characterization steps were carried out at room temperature under ambient laboratory conditions. Current-

95 Voltage characteristics of single-carrier devices were measured using the same semiconductor parameter analyzer as for PhOLED devices. The single-carrier devices measurements were performed under dark and ambient conditions.

Results and discussion

100 **Thermal Properties**

The thermal properties of two complexes **1** and **2** were investigated by differential scanning calorimetry (DSC) and thermal gravimetric analyses (TGA) under a nitrogen atmosphere as shown in Fig. 1 and the data were summarized in Table 1. The

105 DSC data reveal that no glass transition temperature (T$_g$) was observed for both complexes, the melting points (T$_m$) of them are 446 ºC and 482 ºC, respectively. In the TGA study, they exhibit high decomposition temperatures at 417 ºC and 441 ºC respectively with a 5% weight loss (T$_{d5}$). Although the

110 decomposition temperatures of these complexes are slightly lower than their melting points, these values are still much higher than the complexes of Ir(C^N)$_3$ and Ir(C^N)$_2$(L^X) types.[10] This

result proved to be the advantage of these tridentate cyclometalated ligand in terms of thermal stabilities, which can prevent them from decomposing during the process of vacuum deposition as well as device working.[11]
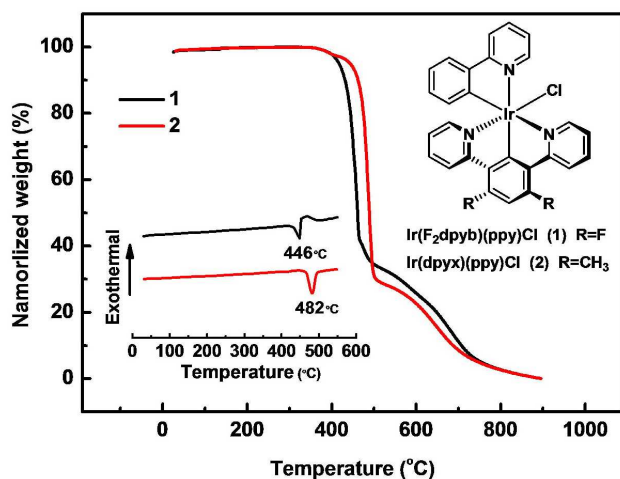

5 **Fig. 1** TGA thermograms of **1** and **2**. Inset: the chemical structure and DSC thermograms of **1** and **2**.
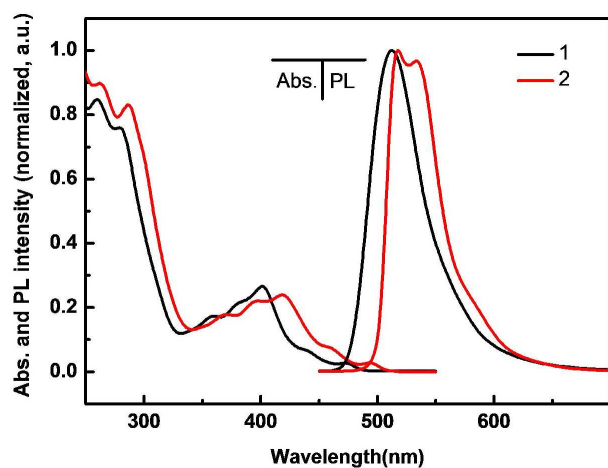

Fig. 2 UV/Vis absorption and photoluminescence (PL) spectra of complexes **1** and **2** in dilute degassed solution.

Photophysical and electrochemical properties

10 Fig. 2 shows the absorption and photoluminescent (PL) spectra of **1** and **2** in degassed dilute CH_2Cl_2 solution at 298K. Intense absorption bands were observed in the ultraviolet part of the spectrum between 240 and 350 nm, assignable to the spin-allowed $^1(\pi-\pi^*)$ transitions of the aromatic moieties. The
15 absorption bands observed at lower energies extending into the region of 350–450 nm that have been assigned to the metal-to-ligand charge transfer (^{1}MLCT). These ^{1}MLCT bands have been attributed to an effective mixing of charge transfer transitions with higher lying spin-allowed transitions on the cyclometalated
20 ligand. This mixing is facilitated by the strong spin-orbit coupling of the Ir(III) center.[12] The weak shoulder peaks extending into the region of 450 to 540 nm were assigned associated with both spin-orbit coupling enhanced $^3(\pi-\pi^*)$ and spin-forbidden ^{3}MLCT transitions, which are inevitable nature for phosphorescent

25 materials.[13] Their absorption edges correspond to S_0-S_1 transition indicate the energy bandgaps (E_g) of complex **1** and **2** which can be assumed to be 2.53 and 2.44 eV. Both the complexes show intensely PL emission in degassed dilute CH_2Cl_2. The emission peaks are 511 nm for **1**, 517 and 534 nm for **2**, and such trend can
30 be rationalized in terms of the electronic effects of the fluorine substituents as follows. F atoms might be expected to lower the energy of all orbitals thought their electron-withdrawing nature, and this effect is larger for the HOMO than for LUMO.[4c] Thus, the transitions shift to higher energy, and the absorption and
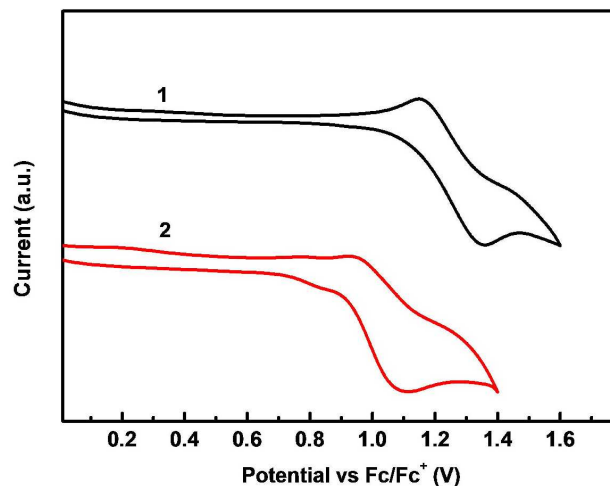35 emission bands of complex **1** are blue-shifted compared with that of complex **2**.

Fig. 3 Cyclic voltammograms of complexes **1** and **2** in DMF for oxidation.

Table1 Physical properties of complexes **1** and **2**.

Complex	1	2
$\lambda_{abs}[nm]sol^{a)}$	473, 441, 401	494, 459, 419
$\lambda_{PL}[nm]sol^{a)}$	511	517, 534
$T_g/T_m/T_d\ [\ ℃]^{b)}$	N/446/417	N/482/441
$HOMO/LUMO[eV]$	-5.57/-3.04	-5.33/-2.89

a) Measured in degassed CH_2Cl_2 solution (10^{-5} M); b) N: Not observed.

The electrochemical properties of these complexes were
40 studied in DMF solution through Cyclic Voltammetry (CV) measurements using ferrocene as the internal standard. Their cyclic voltammograms are shown in Fig. 3. The oxidation process is analogous to removing an electron from the metal-centered HOMO level,[14] therefore the oxidation of complexes **1** and **2** can
45 be assigned to the Ir^{IV}/Ir^{III} oxidation.[11b] Both of them undergoes reversible one-electron oxidation processes and the HOMO levels of complex **1** and **2** are determined to be -5.57 and -5.33eV respectively. In addition, the reduction process is equivalent to adding an electron to the ligand-centered LUMO level. Because
50 no clear reduction wave was observed within the potential window of the cyclic voltammograms, the LUMO energy levels of **1** and **2** were deduced from HOMO energy levels and optical band gaps determined by the onset of absorption using the expression: LUMO=HOMO + E_g, thus the LUMO energy levels
55 are -3.04eV (-5.57+2.53) and -2.89 eV (-5.33+2.44) respectively as shown in Table 1.

Charge carrier injection and transport properties

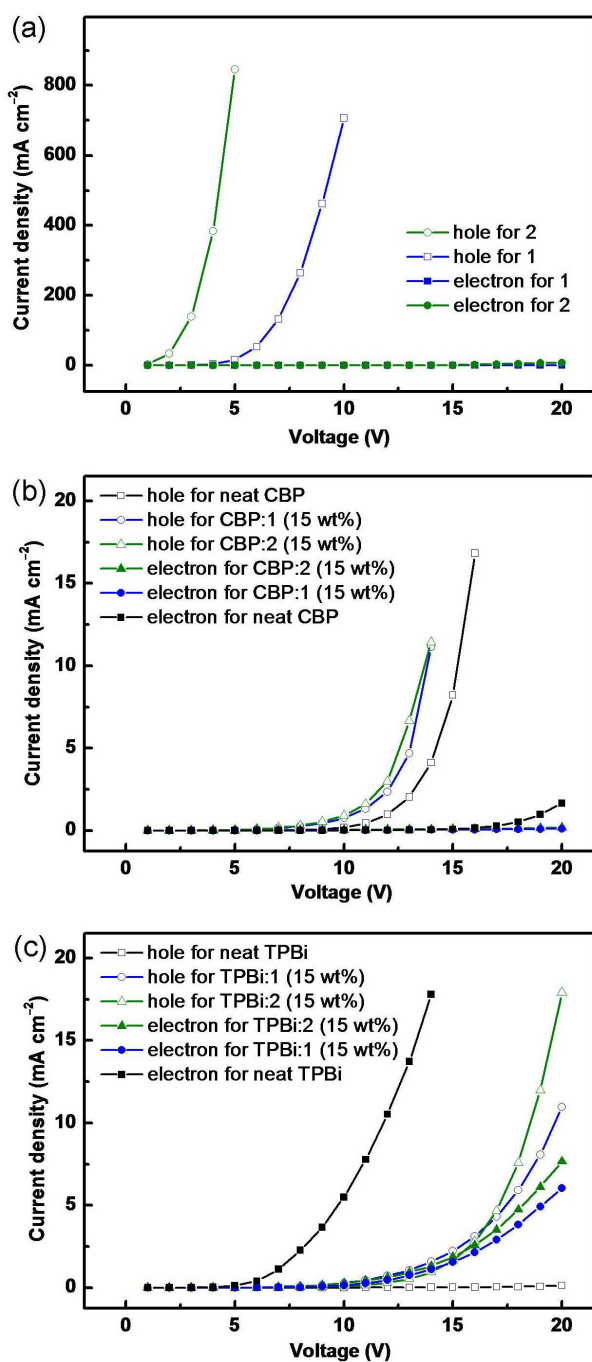Single-carrier devices adopting the two complexes **1** and **2** as the

Fig. 4 Current density versus voltage characteristics of the hole-only and electron-only devices with the active layer based on the neat **1** and **2** films (a), the neat CBP films as well as the doping CBP:**1** or **2** films (b) and the neat TPBi films as well as the doping TPBi:**1** or **2** films (c).

active layer with the structures of [ITO/MoO$_3$ (10 nm)/ **1** or **2** (60 nm)/MoO$_3$ (10 nm)/Al (100 nm)] for hole-only device and [ITO/TPBi (10 nm)/ **1** or **2** (60 nm)/TPBi (10 nm)/LiF (1 nm)/Al (100 nm)] for electron-only device were fabricated. It can be assumed that only single carriers are injected and transported in these devices due to the work function of MoO$_3$ (or the HOMO of TPBi) layers being high (or low) enough to block electron (or hole) injection, while the hole and electron can be easy to inject into the active layer without the energy barrier from the MoO$_3$

and TPBi layer respectively.[15] For comparison, series of devices with the same configurations as the single-carrier devices above, were fabricated by using neat CBP, neat TPBi, CBP doped with **1** or **2** (15 wt%) and TPBi doped with **1** or **2** (15 wt%) as the active layer respectively, instead of neat **1** or **2**.

Among the *I–V* characteristics of four single-carrier devices based on the neat **1** or **2** layer as shown in Fig. 4a, we observe that both the hole current of **1** and **2** are rapidly increased whereas both the electron-only devices exhibit very high threshold voltages. The significant difference between the *I–V* curves of the hole- and electron-only devices based on either complex indicates that both **1** and **2** are the unipolar molecules, which only effectively conduct the hole carriers injected into the organic layer. This similar charge-transporting character of **1** and **2** indicates that the fluorine (F) substituent in the N^C^N is seen to have no substantial influence on the charge transporting property. Likewise, the undoped single-carrier devices of CBP and TPBi (Fig. 4b and 4c) show that CBP and TBPi molecules prefer to accept and transport the hole and electron respectively. Furthermore, it is gratifying, the hole-only devices with the layer of **1** and **2** doped in TPBi not only have much higher current density than the hole-only device with the pure TPBi layer, but show comparable current level with the corresponding electron-only devices. In contrast, the electron-only devices based on CBP:**1** or **2** layer show flat current curves like the base line, which are lower than the curve of the electron-only device with the neat CBP layer. This phenomenon suggests that the dopant **1** and **2** can be used as the media for hole injecting into and transporting in the TPBi host layers while their role in doped CBP layer is just trapping the electron from CBP sites. These results are consistent with our expected bipolar EMLs composed of TPBi and **1** or **2**, in which the dopant (**1** or **2**) and the host (TPBi) molecules can serve as two convenient channels for transporting both holes and electrons, and they will facilitate holes and electrons injection and conduction across the EML by hopping between the adjacent dopant and host molecules respectively, and then achieve balanced charge fluxes, resulting in high device performance.

Characterization of phosphorescent OLEDs

To evaluate the EL performance of complexes **1** and **2** doped in different type host materials, a series of PHOLEDs with an uniform and simple configuration of [ITO/NPB (40 nm)/TCTA (10nm)/emitting layer (30 nm)/TPBI (30 nm)/LiF (0.5 nm)/Al] were fabricated, and the energy diagram of the materials used in the EL device above are shown in Fig. 5a. NPB and TPBi were employed as the hole transport layer (HTL) and electron transport/hole-blocking layer (ETL and HBL), respectively, and TCTA was used as the electron-blocking layer, as well as triplet exciton blocker layer in the PhOLEDs. The films of **1** and **2** doped in TPBi and CBP with the concentration of 15 wt% were adopted as EMLs to fabricate devices **T1** (TPBi:**1**), **T2** (TPBi:**2**), **C1** (CBP:**1**) and **C2** (CBP:**2**) respectively. The devices present bright blue-green and green emission with maximum at ~490 nm for **T1** and **C1** and ~510 nm for **T2** and **C2** at the brightness of 500 cd m^{-2} (Fig. 5b).

The current density-voltage-luminance (*J-V-L*) characteristics of the devices are shown in Fig. 6a, and the EL performance data are summarized in Table 2. All the devices displayed low driving

voltages, and the corresponding current density and luminance exhibited sustained increase upon increasing driving voltage. On the whole, although the **C**-series devices (**C1** and **C2**) showed higher current-density level than **T**-series devices (**T1** and **T2**),
5 the high current of the **C**-series devices could not lead to the higher luminance than that of **T**-series devices, that is, two luminance curves of **T1** and **C1**, **T2** and **C2** are intertwining together, showing the similar luminance level. The luminance of four devices plotted against current density in Fig. 6b gives a
10 more intuitive comparison between **C**- and **T**-series devices, where **T1** and **T2** exhibited much higher luminance than **C1** and **C2** respectively under each current density value. It indicates that there are more balanced hole-electron pairs in **T1** and **T2** benefited from the bipolar EMLs based on TPBi:dopant, which
15 increase the recombination efficiency and harvest more excitons than in the case of CBP:dopant systems.
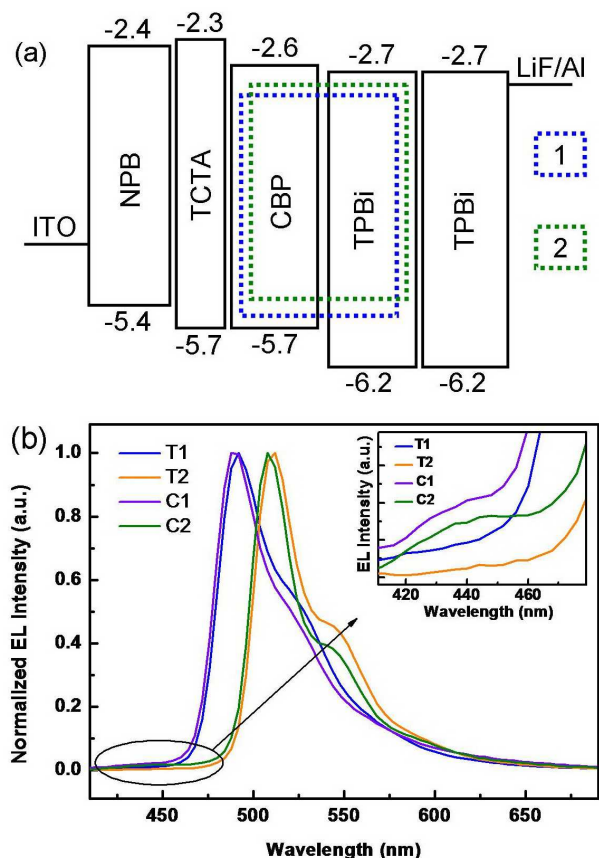

Fig. 5 (a) Proposed energy diagram of the materials used in OLEDs. (b) EL spectra of devices **T1**, **T2**, **C1** and **C2** at the luminance of 500 cd m^{-2}.
The inset in (b) is an enlarged image of the EL curves at the wavelengths
20 from 410 to 480 nm.

Fig. 6c displays the external quantum efficiency (EQE) and power efficiency (PE) plotted with respect to the luminance of all devices and the EL performance data are summarized in Table 2. **T1** and **T2** exhibited much higher EQE and PE than **C1** and **C2**
25 respectively, implying that complex **1** or **2** doped in TPBi is really a much more matched and efficient host-dopant system than the CBP-based doping layer. This may be due to two reasons: Firstly, in **T**-series devices, the hole-transporting dopant material (**1** or **2**) and the electron-transporting host material TPBi compose
30 the bipolar EMLs, leading to a strategy of direct recombination
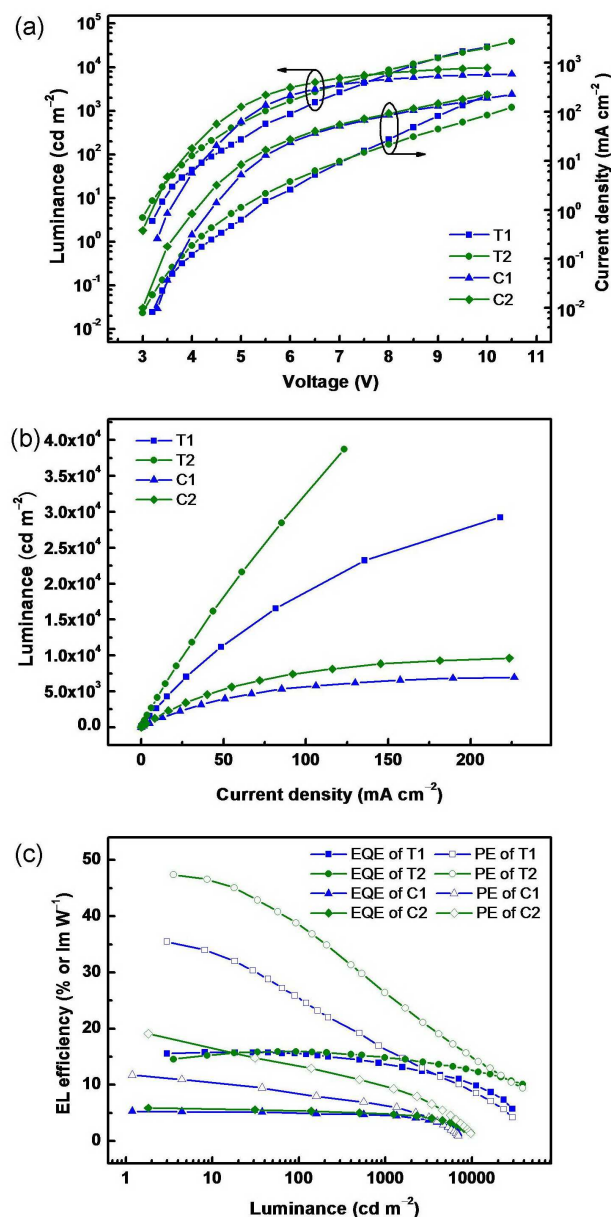

Fig. 6. Current density-voltage-luminance (*J-V-L*) curves (a), luminance-current density curves (b) and power efficiency-luminance-external quantum efficiency curves (c) of devices **T1**, **T2**, **C1** and **C2**.

on the dopant through hole injection into dopant together with the
35 electron injection into host. It ensures a balanced hole-electron current and broadens the exciton-formation zone in their EMLs, consequently achieving higher luminance under the same current density than that in the EMLs of **C**-series devices, where the dominated carriers are the holes depending on the CBP molecules,
40 causing the narrow recombination zone formed close to the ETL interface with the high polaron density, thereby increasing the probability of the TTA and leading to low device efficiency. Secondly, a slight emission at 420-460 nm due to the CBP host plus the dominant peak being detectable in the EL spectrum of
45 **C1** or **C2** respectively (Fig. 5b inset), suggests that part of recombination of injected holes and electrons occurs at the CBP host molecule sites and then the excited energy is incomplete

transfer from CBP to **1** or **2** in the **C**-series devices, even though they employ rather high doping concentration of 15 wt%. Generally, direct charge recombination should be a more effective way to achieve high efficiency in PhOLEDs, because energy losses during the host-dopant energy transfer process can be avoided.[5g]

Hence, **T1** and **T2** logically achieved the EQE (η_e) as high as 15.8 and 16.7 % together with the peak PE (η_p) values of 35.5 and 47.4 lm W^{-1}, which maintain the high level of 14.5 and 16.1 % & 19.2 and 30.6 lm W^{-1} respectively, at rather high and practical luminance of 500 cd m^{-2} with the low driving voltages of less than 6 V. These are rather high values, which show almost a twofold enhancement over the most efficient PhOLEDs ever

reported based on the iridium complexes with terdentate ligands,[4] where the conventionally used CBP or TCTA with the primary hole-transporting ability are employed as the host material. Thus, obviously, an appropriate selection of host and dopant materials plays a significant role in the design of highly efficient PhOLEDs. Furthermore, it is worth mentioning that the EL performance of **T1** based on complex **1** have exceeded those of the high-performance blue-green PhOLEDs reported based on the phosphorescent complexes containing two bidentate cyclometallating ligands with the structrural class of Ir(C^N)$_2$(L^X),[16] hence offering a wider diversity of substitution and extend scope for manipulating the optoelectronic properties of the iridium-based phosphorescent emitters.

Table 2 Electroluminescent properties of the devices.[a]

Device	V_{on}/V	L_{max}/cd m^{-2}(V at L_{max})	η_e[b]/%	η_p[b]/lm W^{-1}	EL emisison peak, CIE (x,y)[c]
T1	3.2	29250 (10.0)	15.8, 15.5, 14.5	35.5, 25.6, 19.2	492, (0.20, 0.53)
T2	3.0	38760 (10.5)	16.7, 16.7, 16.1	47.4, 38.5, 30.6	512, (0.25, 0.65)
C1	3.3	6970 (10.5)	5.3, 5.0, 4.8	11.8, 8.5, 7.2	488, (0.19, 0.49)
C2	3.0	9640 (10.0)	5.9, 5.5, 5.0	19.1, 13.6, 10.9	508, (0.24, 0.64)

[a]Abbreviation: V_{on}: Turn-on voltage (Recorded at 1 cd m^{-2}). L_{max}: Maximum luminance. η_e: External quantum efficiency. η_p: Power efficiency. [b]In the order of maximum, then values at 100 and 500 cd m^{-2}. [c]Measured at 500 cd m^{-2}

Conclusions

In summary, the most efficient PhOLEDs based on the iridium complexes with the N^C^N-coordinated terdentate ligands have been realized. Here, the appropriate selection of a prominent electron-transport molecule TPBi as a host to matching the [Ir(N^C^N)(N^C)X]-type phosphorescent dopant emitters that possess the obvious hole-transport ability, plays a critical role in the remarkable EL-performance improvement on this series of PhOLEDs previously reported. The bipolar host-dopant systems in this study, that is, the dopant and host molecules indeed dominate the hole/electron transport respectively, ensures the balanced and enough charge fluxes, and thus allowing for exciton formation and recombination directly on the dopant sites those distributed throughout the corresponding EMLs, which results in low-voltage PHOLEDs with high and stable EL efficiencies. More importantly, as a result of their desired EL performance, which is at least comparable, and in some cases superior to that obtained with some Ir(C^N)$_3$ and Ir(C^N)$_2$(L^X) complexes, these [Ir(N^C^N)(N^C)X]-type phosphorescent emitters might become an emerging research activity in testing phosphors for OLEDs parallels to the bibentate ligand-based iridium complexes, together finding application in full-color display and solid state lighting.

Acknowledgements

Notes and references

State Key Laboratory of Supramolecular Structure and Materials, Jilin University, Changchun 130012, P. R. China, E-mail: yuliu@jlu.edu.cn *(Yu Liu) and* zhangjingy@jlu.edu.cn *(Jingying Zhang).*

1   (a) M. A. Baldo, D. F. O'Brien, Y. You, A. Shoustikov, S. Sibley, M. E. Thompson and S. R. Forrest, *Nature*, 1998, **395**, 151; (b) M. A. Baldo, S. Lamansky, P. E. Thompson and S. R. Forrest, *Appl. Phys. Lett.*, 1999, **75**, 4.

2   (a) S. Lamansky, P. Djurovich, D. Murphy, F. Abdel-Razzaq, H. E. Lee, C. Adachi, P. E. Burrows, S. R. Forrest and M. E. Thompson, *J. Am. Chem. Soc.*, 2001, **123**, 4304; (b) S. Lamansky, P. Djurovich, D. Murphy, F. Abdel-Razzaq, R. Kwong, I. Tsyba, M. Bortz, B. Mui, R. Bau and M. E. Thompson, *Inorg. Chem.*, 2001, **40**, 1704; (c) M. K. Nazeeruddin, R. Humphry-Baker, D. Berner, S. Rivier, L. Zuppiroli and M. Graetzel, *J. Am. Chem. Soc.*, 2003, **125**, 8790; d) A. Tsuboyama. H. Iwawaki, M. Furugori, T. Mukaide, J. Kamatani, S. Igawa, T. Moriyama, S. Miura, T. Takiguchi, S. Okada, M. Hoshino and K. Ueno, *J. Am. Chem. Soc.*, 2003, **125**, 12971.

3   L. X. Xiao, Z. J. Chen, B. Qu, J. X. Luo, S. Kong, Q. H. Gong and J. Kido, *Adv. Mater.*, 2011, **23**, 926.

4   (a) M. Ashizawa, L. Yang, K. Kobayashi, H. Sato, A. Yamagishi, F. Okuda, T. Harada, R. Kuroda and M. Haga, *Dalton, Trans.*, 2009, 1700; (b) J. Kuwabara, T. Namekawa, M. Haga and T. Kanbara, *Dalton, Trans.*, 2012, **41**, 44; (c) P. Brulatti, R. J. Gildea, J. A. K. Howard, V. Fattori, M. Cocchi and J. A. G. Williams, *Inorg. Chem.*, 2012, **51**, 3813.

5   (a) S. O. Jeon, K. S. Yook, C. W. Joo and J. Y. Lee, *Adv. Mater.*, 2009, **19**, 3644; (b) S. O. Jeon, K. S. Yook, C. W. Joo and J. Y. Lee, *Adv. Mater.*, 2010, **22**, 1872; (c) H.-H. Chou and C.-H. Cheng, *Adv. Mater.*, 2010, **22**, 2468; (d) S. L. Gong, Y. H. Chen, J. J. Luo, C. L. Yang, C. Zhong, J. G. Qin and D. G. Ma, *Adv. Func. Mater.*, 2011, **21**, 1168; (e) C.-H. Fan, P. P. Sun, T.-H. Su and C.-H. Cheng, *Adv. Mater.* 2011, **23**, 2981; (f) T. Peng, G. M. Li, K. Q. Ye, C. G. Wang, S. S. Zhao, Y. Liu, Z. M. Hou and Y. Wang, *J. Mater. Chem. C*, 2013, **1**, 2920; (g) A. Wada, T. Yasuda, Q. Zhang, Y. S. Yang, I. Takasu, S. Enomoto and C. Adachi, *J. Mater. Chem. C*, 2013, **1**, 2404.

6   (a) T. Tsuzuki and S. Tokito, *Adv. Mater.*, 2007, **19**, 276; (b) R. J. Holmes, B. W. D'Andrade, S. R. Forrest, X. Ren, J. Li and M. E. Thompson, *Appl. Phys. Lett.*, 2003, **83**, 3818; (c) Q. Wang, J. Q. Ding, D. G. Ma, Y. X. Cheng, L. X. Wang, X. B. Jing and F. S. Wang, *Adv. Func. Mater.*, 2009, **19**, 84. (d) H. B. Wu, G. J. Zhou, J. H. Zou, C. –L. Ho, W. –Y. Wong, W. Yang, J. B. Peng and Y. Cao, *Adv. Mater.*, 2009, **21**, 4181.

7   (a) S. Takizawa, V. A. Montes and P. Anzenbacher Jr., *Chem. Mater.*, 2009, **21**, 2452; (b) Y.-H. Kim, W. Y. Kim and C.-B. Moon, *J. Appl.*

Phys. 2011, **110**, 034501; (c) Z. W. Liu, M. G. Helander, Z. B. Wang and Z. H. Lu, *Org. Electron.*, 2013, **14**, 852.

8 G. F. He, M. Pfeiffer, K. Leo, M. Hofmann, J. Birnstock, R. Pudzich and J. Salbeck, *Appl. Phys. Lett.*, 2004, **85**, 3911.

5 9 S. G. Jung, Y. J. Kang, H. S. Kim, Y. H.Kim, C. L. Lee, J. J. Kim, S. K. Lee and S. K. Kwon, *Eur. J. Inorg. Chem.*, 2004, **17**, 3415.

10 (a) F. Kessler, Y. Watanabe, H. Sasabe, H. Katagiri, Md. K. Nazeeruddin, M. Grätzela and J. Kido, *J. Mater. Chem. C*, 2013, **1**, 1070; (b) S. Mulani, M. Xiao, S. J. Wang, Y. W. Chen, J. B. Peng and
10 Y.13. Meng, *RSC Adv.*, 2011, **21**, 4983.

11 (a) C.-L. Ho, W.-Y. Wong, Q. Wang, D. G. Ma, L. X. Wang and Z. Y. Lin, *Adv. Funct. Mater.*, 2008, **18**, 928; (b) G. P. Tan, S. M. Chen, N. Sun, Y. H. Li,D. Fortin,W.-Y. Wong, H.-S. Kwok, D. G. Ma, H. B. Wu, L. X. Wang and P. D. Harvey, *J. Mater. Chem. C*, 2013, **1**, 808.

15 12 (a) J. H. Yao, C. Zhen, K. P. Loh and Z. K. Chen, *Tetrahedron*, 2008, **64**, 10814; (b) L. Q. Chen, H. You, C. L. Yang, X. W. Zhang, J. G. Qin and D. G. Ma, *J. Mater. Chem.*, 2006, **16**, 3332; (c) S. Lamansky, P. Djurovich, D. Murphy, F. Abdel-Razzaq, H. F. Lee, C. Adachi, P. E. Burrows, S. R. Forrest and M. E. Thompson, *J. Am. Chem. Soc.*,
20 2001, **123**, 4304;

13 (a) T. Peng, H. Bi, Y. Liu, Y. Fan, H. Z. Gao, Y. Wang and Z. M. Hou, *J. Mater. Chem.*, 2009, **19**, 8072; (b) M. G. Colombo, A. Hauser and H. U. Gudel, *Inorg. Chem.*, 1993, 32, 3088; (c) M. G. Colombo, T. C. Brunold, T. Riedener, H. U. Gudel, M. Fortsch and H.-B. Burgi,
25 *Inorg. Chem.*, 1994, **33**, 545.

14 (a) V. K. Rai, M. Nishiura, M. Takimoto and Z. M. Hou, *J. Mater. Chem. C*, 2014, **2**, 5317; (b) X. Li, Z. Chen, Q. Zhao, L. Shen, F. Li, T. Yi, Y. Cao and C. Huang, *Inorg. Chem.*, 2007, **46**, 5518; (c) M. Velusamy, K. R. J. Thomas, C.-H. Chen, J. T. Lin, Y. S. Wen, W.-T.
30 Hsieh, C.-H. Lai and P.-T. Chou, *Dalton Trans.*, 2007, 3025; (d) J. Li, P. I. Djurovich,B. D. Alleyne, M. Yousufuddin, N. N. Ho, J. C. Thomas, J. C. Peters, R. Bau and M. E. Thompson, *Inorg. Chem.*, 2005, **44**, 1713.

15 (a) M. Kröger, S. Hamwi, J. Meyer, T. Riedl, W. Kowalsky and A.
35 Kahn, *Org. Electron.*, 2009, **10**, 932; (b) W. Jiang, L. Duan, J. Qiao, G. Dong, L. Wang and Y. Qiu, *Org. Lett.,* 2011, **13**, 3146; (c) C. J. Zheng, J. Ye, M. F. Lo, M. K. Fung, X. M. Ou, X. H. Zhang and C. S. Lee, *Chem. Mater.,* 2012, **24**, 643; (d) K. Wang, S. P. Wang, J. B. Wei, S. Y. Chen, D. Liu, Y. Liu and Y. Wang, *J. Mater. Chem. C*,
40 2014, **2**, 6817.

16 (a) H.-J. Seo, M. Song, S.-H. Jin, J. H. Choi, S.-J. Yuna and Y.-I. Kim, *RSC Adv.*, 2011, **1**, 755; (b) Y.-C. Zhu, L. Zhou, H.-Y. Li, Q.-L. Xu, M.-Y. Teng, Y.-X. Zheng, J.-L. Zuo, H.-J. Zhang, and X.-Z. You. *Adv. Mater.*, 2011, **23**, 4041; (c) L. J. Deng, T. Zhang, R. J. Wang
45 and J. Y. Li, *J. Mater. Chem. C*, 2012, **22**, 15910; (d) K. Chao, K. Z. Shao, T. Peng, D. X. Zhu, Y. Wang, Y. Liu, Z. M. Su and M. R. Bryce, *J. Mater. Chem. C*, 2013, **1**, 6800.